Impact of Receiver Thermal Noise and PLL RMS Jitter in Radar Measurements

Zeeshan Ali, *Graduate Student Member, IEEE*, Mostafa Elsayed, Girish Tiwari, Meraj Ahmad, Julien Le Kernec, *Senior Member, IEEE*, Hadi Heidari, *Senior Member, IEEE*, and Shalabh Gupta

***Abstract*—The accuracy of range and velocity measurements relies on the characteristics of the hardware blocks employed within a radar system. In particular, the two crucial blocks in a radar system are the low noise amplifier (LNA) located at the front of the receiver chain and the phase-locked loop (PLL) used as a signal generator. Thus, the predominant noise sources in the radar system are the receiver's thermal noise (primarily influenced by the LNA) and the RMS jitter of the PLL. The presence of noise in these blocks causes uncertainties in the radar measurements. This work derives the formulation of standard deviation for range and velocity uncertainties for frequency-modulated continuous wave (FMCW) and stepped-frequency continuous wave (SFCW) radars and further validates it through real-world measurement results from a radar in X-band. The study primarily examines the effect of parameters such as the RMS jitter and settling time of the signal generator, along with the thermal noise in the receiver on the radar range and velocity measurement. The conclusion drawn from the study is that applications requiring a rapid measurement time with a specified level of accuracy necessitate the integration of a fast-settling PLL in a radar system. Ultimately, the relationship of the specifications of these essential components in the measurement accuracy in radars used in Industry 4.0 can help the designer in developing a robust radar system.**

***Index Terms*—FMCW, fractional-N synthesizer, phase noise, PLL, radar, range, RMS jitter, SFCW, settling time.**

I. Introduction

Monolithic system-level integration of radar chips has become cost-effective due to the advancements in semiconductor technology. The frequency modulated continuous wave (FMCW) and stepped frequency continuous wave (SFCW) radars have thus gained popularity, enabling various applications in the microwave range and imaging systems [1]-[4]. In both radar systems, signal generation stands out as the pivotal component. The signal generation in the radar system can be carried out using a digital-to-analog converter (DAC) driving a voltage-controlled oscillator (VCO) or an integer-N phase-locked loop (PLL) [5]-[6]. Further, to improve the frequency resolution of the DAC-based signal generator, a direct digital synthesizer (DDS) along with a PLL is used [7]-[8]. The fractional-N PLL architecture is the preferred method for successfully integrating two-point modulation (TPM) into scalable CMOS technologies, offering the highest level of modulation capability [9]. This work focuses on the signal generator based on fractional-N PLL.

The measurement accuracy in a radar system will be constrained by the RMS jitter and settling time of the PLL. The dependence of these parameters on the standard deviation of range and velocity would give an estimate of the specifications of the PLL required in developing a radar system. On the other hand, measurement accuracy is also affected by the receiver's thermal noise. A fast-settling PLL would cater for the requirement of high accuracy in the measurement when considering the effects of the thermal noise in the receiver and the RMS jitter of the PLL.

Fig. 1 depicts a simple model of an FMCW homodyne radar front-end to measure the target range and velocity. The round trip time t_d has the target range information as $t_d = 2R/c_o$, where R is the target range and c_o is the speed of light. The transmitted signal at time t is multiplied by the signal at an earlier time t_d by the mixer. The output phase of the radar signal ($\phi_{out}(t)$) after the low-pass filter (LPF) essentially corresponds to the difference in PLL output phases of the transmitter ($\phi(t)$) and its time-delayed version ($\phi(t - t_d)$). The low-pass filtered output is then digitally processed after passing through an analog-to-digital converter (ADC).

A phase variance is observed at the receiver output by anomalies such as the PLL RMS jitter, receiver thermal noise, quantization noise of ADC, sampling clock jitter, and supply-induced noise. This work mainly focuses on the contribution of receiver thermal noise and the PLL RMS jitter in the inaccuracy. It is shown in [10] that the variance of the range measurement in FMCW radar has a higher degree of dependence on receiver thermal noise than the PLL phase noise for far-field objects. However, the mathematical expressions derived here in this work provide a clearer picture of individual contributions of receiver thermal noise and PLL RMS jitter on radar measurement, compared to the work in [10].

In the works of [10], [11], [12], [13], [14], radar systems, including the VCO and PLL phase noise, were introduced. [10], [11] utilized an Ornstein–Uhlenbeck (OU) process to model VCO phase noise, while [12] employed an innovative additive coloured noise (ACN) method to model PLL phase noise. [13] employed Leeson's equation for oscillator phase noise modelling, and [14] utilized a filter-based technique

This work was supported in part by Qualcomm donation and the National Center of Excellence in Technologies for Internal Security (NCETIS), India, through the student scholarship. (Corresponding author: Zeeshan Ali.)

Zeeshan Ali was with the Department of Electrical Engineering, Indian Institute of Technology Bombay, Mumbai 400076, India. He is now currently with James Watt School of Engineering, University of Glasgow, Glasgow G12 8QQ, U.K. (e-mail: ali.zeeshan@glasgow.ac.uk).

Girish Tiwari, and Shalabh Gupta are with the Department of Electrical Engineering, Indian Institute of Technology Bombay, Mumbai 400076, India (e-mail: girishtiwari@ieee.org, shalabh@ee.iitb.ac.in).

Mostafa Elsayed, Meraj Ahmad, Julien Le Kernec and Hadi Heidari are with James Watt School of Engineering, University of Glasgow, Glasgow G12 8QQ, U.K. (2700227e@student.gla.ac.uk; meraj.ahmad@glasgow.ac.uk.)

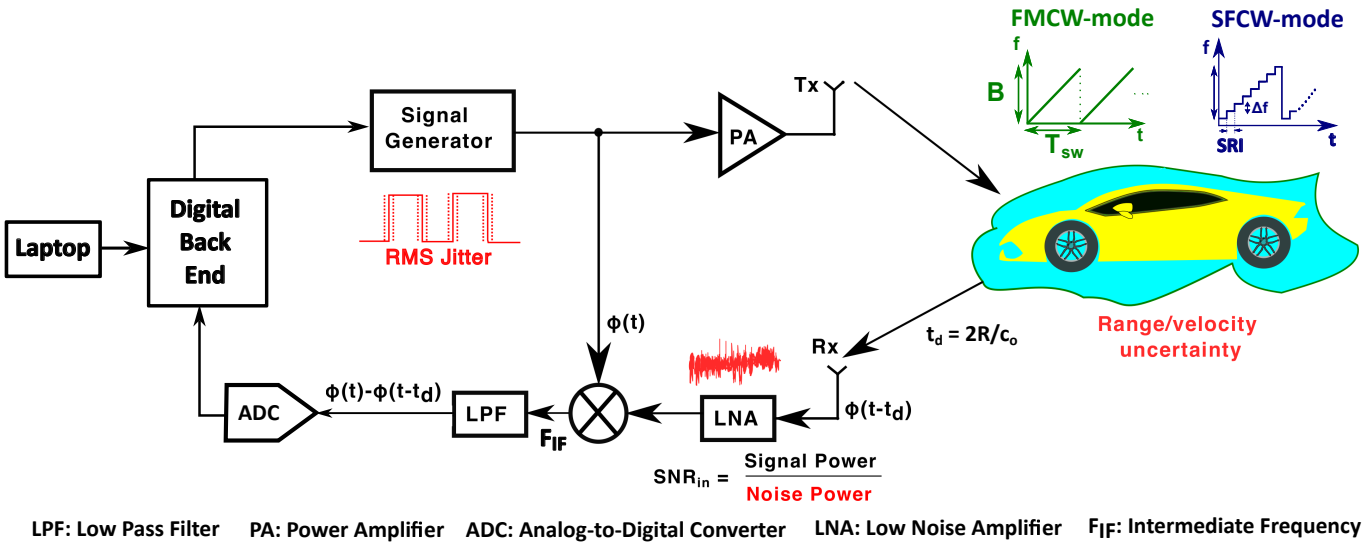

Fig. 1. A simple model of a homodyne radar system to estimate the range and velocity of a target.

for PLL noise modelling. Notably, these works lacked a clear representation of measurement uncertainty in the radar system based on overall PLL RMS jitter. The VCO phase noise undergoes high-pass filtering within the closed loop in PLL and the "close-in" phase noise of the VCO is reduced significantly by the action of the PLL [15]. In an effort to mitigate the ambiguity associated with the dependence of VCO on the PLL phase noise, the literature often reports the RMS jitter of the PLL. The formulation presented in this paper establishes an explicit relationship between PLL RMS jitter, receiver thermal noise, and radar measurement uncertainties.

Accurate speed control is crucial in automation, impacting productivity, quality, and process reliability. Radar systems are frequently utilized in the automation sector in Industry 4.0. This study focuses on understanding radar anomalies' impact on velocity measurement, aiding in selecting appropriate specifications of the components in the radar systems for dependable outcomes in various industrial settings.

While FMCW radars are extensively utilized in various applications, SFCW radars remain the preferred choice in applications such as GPR, remote sensing, biomedical, and other imaging applications [16], [17]. There is a lack of available literature that addresses the investigation of ambiguity caused by noise in SFCW radars. The main contributions of this work are:

1) To present a clearer dependence of range uncertainties in a radar system on receiver thermal noise and PLL RMS jitter.
2) To comprehensively address the impact of receiver thermal noise and RMS jitter in the PLL on the accuracy of velocity measurements in radar systems.
3) To present the measurement uncertainty relation to the thermal noise and PLL RMS jitter in SFCW radar systems.
4) We present that a meticulous exploration of these noise-related influences becomes imperative for selecting an appropriate chirp time for FMCW radar or a suitable stepped repetitive interval (SRI) for SFCW radar. This choice aims to mitigate uncertainties in range and velocity measurements effectively.

This work investigates the effects of receiver thermal noise on the range and velocity uncertainty in FMCW and SFCW radar systems in Section II. The effect of PLL RMS jitter on both radar systems' range and velocity accuracy is explored in Section III. The theory presented in these sections is validated by measurement results, presented in Section IV. Finally, Section V concludes this paper.

II. Effect of Thermal Noise in the Receiver

The signal at the receiver output after LPF represented as (1), will have the signal power $V_0^2/2$.

$$V_o(t) = V_0.cos(2\pi f_o t + \phi_{out}(t)) \tag{1}$$

The output frequency f_o is related to the bandwidth (B), sweep time (T_{sw}), target range (R), and speed of the light (c_o) as

$$f_o = \frac{2.B.R}{T_{sw}.c_o} \tag{2}$$

The noise power of the signal given in (1), can be written as

$$\sigma_V = \sqrt{\frac{V_0^2}{2(SNR)_o}} \tag{3}$$

where $(SNR)_o$ is signal-to-noise ratio at the output of receiver, which can be further expressed in terms of input signal-to-noise ratio, $(SNR)_i$, and receiver noise factor (F), as

$$(SNR)_o = \frac{(SNR)_i}{F} \tag{4}$$

The signal slope at the zero crossings is given as

$$\left|\frac{dV_o}{dt}\right|_{V_o(t)=0} = 2\pi f_o V_0 \tag{5}$$

Using (3), (4), (5), and propagation of uncertainty (PoU), the RMS timing jitter σ_t can be found as

$$\sigma_t = \frac{\sigma_V}{\left|\frac{dV_o}{dt}\right|_{V_o(t)=0}} = \frac{1}{2\pi f_o}\sqrt{\frac{F}{2(SNR)_i}} \tag{6}$$

Using (6) as a baseline equation, we now find the range and velocity uncertainty because of the noise in the receiver in FMCW and SFCW radar in the subsequent subsections.

A. FMCW

This section is based on the assumptions mentioned below.

1) The sweep time T_{sw} is considered after the PLL in the FMCW radar has reached its steady state.
2) The flicker noise is neglected since the FMCW radars have significant intermediate frequency (IF).

With output period represented as $T_o = 1/f_o$, and exploiting the fact that two successive output periods are uncorrelated for white noise sources, we get $\sigma_{T_o} = \sqrt{2}.\sigma_t$ [10]. Using the above information, the standard deviation of one output period is obtained as

$$\sigma_{T_o} = \frac{1}{2\pi f_o}\sqrt{\frac{F}{(SNR)_i}} \tag{7}$$

The standard deviation at the output frequency f_o can be found using (7) and PoU, as

$$\sigma_{f_o} = \sigma_{T_o}.f_o^2 = \frac{f_o}{2\pi.}\sqrt{\frac{F}{(SNR)_i}} \tag{8}$$

With f_o being a stochastic process, the standard deviation in (8) is degraded by a factor of $\sqrt{1/n}$, where n is the number of oscillations of output period at the receiver output, given as $n = T_{sw}f_o$ [10]. The obtained standard deviation of IF frequency averaged over one sweep is represented by

$$\sigma_{\overline{f_o}} = \frac{1}{2\pi}\sqrt{\frac{f_o.F}{T_{sw}.(SNR)_i}} \tag{9}$$

Using (2), (9) and PoU, we get

$$\sigma_R = \frac{T_{sw}.c_o}{2B}.\sigma_{\overline{f_o}} = \frac{1}{2\pi}\sqrt{\frac{c_o.F.R}{2B.(SNR)_i}} \tag{10}$$

The input SNR at the matched receiver in terms of transmitted signal energy (E_T), the gain of the transmitter and receiver antennae (G), wavelength in the medium (λ), radar scattering cross-section of the object (RCS), range of the object (R), Boltzmann constant (k_B), system temperature (T_0) and the system noise factor (F) is represented as (11) [18].

$$(SNR)_i = \left[\frac{E_T.G^2}{k_B.T_o.F}\right].\left[\frac{\lambda^2.(RCS)}{(4\pi)^3.R^4}\right] \tag{11}$$

The transmitted signal energy, E_T, for a signal of power $P_T(t)$ for duration τ is given as

$$E_T = \int_0^\tau P_T(t)dt \tag{12}$$

TABLE I
CONFIGURABLE RADAR SYSTEM PARAMETERS

Carrier Frequency	9.5 GHz
Average Transmitted Power	20 dBm
Total Noise Figure	5 dB
Bandwidth	1 GHz
Sweep Time*	50 μs
Gain of Tx and Rx Antenna	10 dB
No of steps (SFCW)*	64

* Configurable

The average transmitting power over a sweep time is given as

$$\hat{P_T} = \frac{E_T}{T_{sw}} \tag{13}$$

1) Range uncertainty: Using (11) and (13) in (10), the variance in range (σ_R^2) in terms of sweep time (T_{sw}), range (R), and centre frequency (f_c) can be found as

$$\sigma_R^2 = \frac{8\pi k_B.T_o.F^2.f_c^2.R^5}{B.\hat{P_T}.T_{sw}.G^2.c_o.(RCS)} \tag{14}$$

The following conclusions can be drawn from (14):

1) $\sigma_R \propto \frac{R^{5/2}}{\sqrt{T_{sw}}}$ signifies that to improve the standard deviation in the range estimation, T_{sw} should be judiciously chosen to be above a minimum T_{sw} where the value of change in σ_R is insignificant,
2) a trade-off exists between measurement time, ADC sampling rate and accuracy,

2) Velocity uncertainty: Similar to the analysis done for estimating range uncertainty, the velocity uncertainty can also be estimated. A minimum of two chirps are essential to estimate the velocity of an object [19]. The velocity is calculated based on the phase difference information captured from the same frequency from the two different chirps. The target would have travelled (ΔR) at these two instants, resulting in the phase difference. For two chirps from the transmitter with individual sweep time T_{sw}, the velocity is evaluated based on the phase difference sensed at the receiver given as

$$\upsilon = \frac{\lambda.\Delta\phi}{4\pi.T_{sw}} \tag{15}$$

where λ is the wavelength and $\Delta\phi$ is the phase difference observed at the receiver. The variation in range affects the phase difference observed at the receiver, thus, $\Delta\phi$ depends on the range accuracy given in (14).

Using (15) and PoU, the standard deviation in velocity in terms of standard deviation in $\Delta\phi$ can be found as

$$\sigma_\upsilon = \frac{\lambda}{4\pi.T_{sw}}.\sigma_{\Delta\phi} \tag{16}$$

The derivations for velocity uncertainty estimation are valid under the assumption that ΔR_{max} is already known. One example is the displacement in the stepper motor head of an automated machine like a 3D printer or a surgical robot.

The change in phase is related to the displacement (ΔR) as

$$\Delta\phi = 2\pi f_o\frac{2\Delta R}{c_o} = \frac{4\pi.f_o.\upsilon.T_{sw}}{c_o} \tag{17}$$

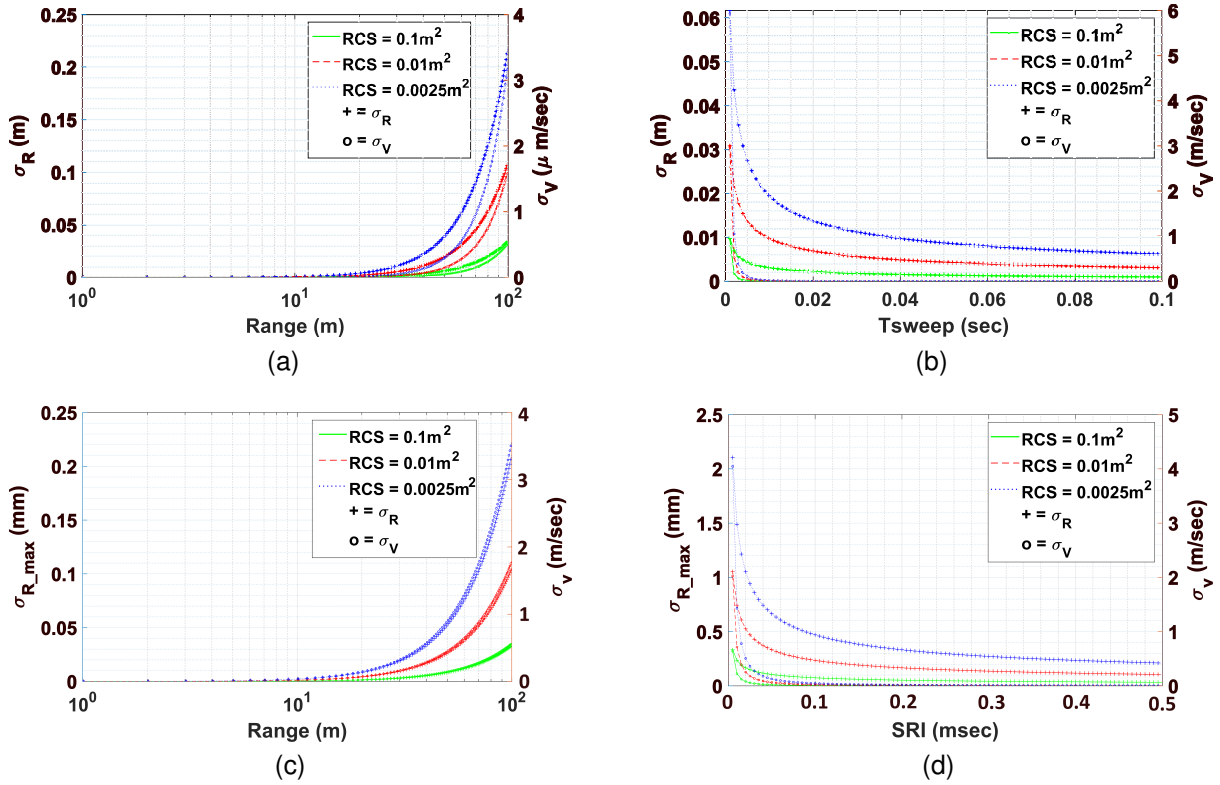

Fig. 2. Effect of thermal noise in the receiver in FMCW radar: Range and velocity uncertainty vs (a) range; (b) sweep time, for $R = 10m$. Effect of thermal noise in the receiver in SFCW radar: Range and velocity uncertainty vs (a) range; (b) SRI, for $R = 10m$.

Using (2), (17), and PoU, we get the standard deviation in the observed phase difference, in terms of the standard deviation in range, as

$$\sigma_{\Delta\phi} = \frac{4\pi f_o}{c_o}\sigma_R = \frac{8\pi.B.R}{c_o^2.T_{sw}}.\sigma_R \tag{18}$$

The variance in the velocity estimation (σ_v^2) in terms of T_{sw}, R can be found using (18) and (14) as

$$\sigma_v^2 = \frac{16\pi.k_B.T_0.F^2.B.R^7}{c_o^3.T_{sw}^5.\hat{P}_t.G^2.(RCS)} \tag{19}$$

Equation (19) implies that improving standard deviation in velocity estimation relies on carefully selecting T_{sw}, keeping the relation $\sigma_v \propto \frac{R^{7/2}}{T_{sw}^{5/2}}$ in mind. This highlights the crucial trade-off between measurement time and accuracy, emphasizing the need for a thoughtful balance between the two factors.

Table I presents the radar system parameters employed in this work. $Matlab$ simulations were conducted to assess range uncertainty and velocity uncertainty, as indicated in equations (14) and (19), respectively. The simulations involved varying range and sweep time (T_{sw}) across three different RCS values, as depicted in Fig. 2a and Fig. 2b, respectively. Notably, the standard deviation in both range and velocity rises for far-field targets and smaller RCS values. Conversely, the standard deviation in range and velocity decreases as T_{sw} increases.

B. SFCW

The SFCW operate with N stepped frequency swept over the bandwidth (B) with a discrete frequency step Δf (=$\frac{B}{N}$). A simple model of an SFCW radar system is shown in Fig. 1. The SRI is the amount of time spent in one frequency step. The entire frequency band is swept in N*SRI. If N frequencies are transmitted in an SFCW radar, then phase ϕ_{1-N} are represented as $\phi_k = 4\pi f_k R/c$, where $k \in [1, N]$. Using this baseline method, we perform the range and velocity uncertainty analysis in an SFCW radar. The radar in Table I can be configured to operate as a stepped frequency with 64 steps with SRI of 50 μs/64 $\approx$ 0.78 μs.

1) Range uncertainty: In SFCW, the phase difference corresponding to two subsequent frequencies from the first till N^{th} frequency in the tuning range is given as

Assuming the target is stationary, the RMS value of the phase difference corresponding to all the frequencies is denoted as $\Delta\phi_{rms} = 4\pi R\Delta f/c$. The range in terms of the RMS value of the phase difference corresponding to two subsequent frequencies is denoted as

$$R = \frac{N.c.\Delta\phi_{rms}}{4\pi B} \tag{20}$$

Using (20) and PoU, we obtain the standard deviation in range in terms of the standard deviation of the RMS value of the phase difference corresponding to two subsequent frequencies

$$\sigma_R = \frac{N.c}{4\pi B}.\sigma_{\Delta\phi_{rms}} \tag{21}$$

Representing $\sigma_{\Delta\phi_{rms}}$ in terms of RMS timing jitter of the received signal σ_t given in (6), we get

$$\sigma_{\Delta\phi_{rms}} = 2\pi f_k\sigma_t = \sqrt{\frac{F}{2(SNR)_i}} \tag{22}$$

Putting (11) and (22) in (21), we get the maximum variance in range as

$$\sigma^2_{R\_max} = \frac{2\pi N.k_B.T_o.F^2.R^4.f^2_{max}}{B^2.\hat{P}_t.(SRI).G^2.(RCS)} \tag{23}$$

Below are the conclusions drawn from (23):

1) $\sigma_{R\_max} \propto \frac{R^2 f_{max}}{\sqrt{SRI}}$ implies that reducing standard deviation in range uncertainty necessitates a higher SRI. However, this elongates measurement time unnecessarily. Hence, the goal for any radar system should be to maintain a minimal SRI that causes negligible alterations in range variation.
2) The dwell time in one frequency should be at least 2x times the PLL settling time [20]. This demands a faster settling time of the signal generator,
3) With fixed B, a trade-off exists between measurement time (N∗SRI), maximum range ambiguity ($R_{max} = \frac{c_o}{2\Delta f}$), and accuracy,

2) Velocity uncertainty: Two frames transmitted can establish a relation for the variation in velocity error. The consecutive phase difference, ($\phi_d = \phi_{2,1} - \phi_{1,1}$), at one transmitted frequency, where the first index is the frame number and the second index is the frequency, is represented as

$$\phi_d = \frac{4\pi N f_1 \Delta R}{c_o} = 2\pi N f_1 \Delta t \tag{24}$$

where $\Delta t = \frac{2\Delta R}{c_o}$. The velocity for an SFCW case in terms of ϕ_d and SRI is represented as

$$\upsilon = \frac{\lambda.\phi_d}{4\pi N.(SRI)} \tag{25}$$

After applying PoU in (25) we get

$$\sigma_\upsilon = \frac{\lambda}{4\pi N.(SRI)}.\sigma_{\phi_d} \tag{26}$$

With the same assumption made in velocity uncertainty estimation stated in Section II-A2, and using (6), and (24), the σ_{ϕ_d} in relation to variation in the RMS timing jitter of the received signal $\sigma_{\Delta t}$ can be given as

$$\sigma_{\phi_d} = 2\pi N f_1 \sigma_{\Delta t} = N.\sqrt{\frac{F}{2.(SNR)_i}} \tag{27}$$

Using (26) and (27), the variance in velocity, which, when averaged over N number of stepped frequencies, results in

$$\sigma^2_\upsilon = \frac{\pi.k_B.T_o.F^2.R^4}{\hat{P}_t.N^2.(SRI^3).G^2.(RCS)} \tag{28}$$

The following observations can be drawn from the study:

1) $\sigma_\upsilon \propto \frac{R^2}{SRI^{1.5}}$, demands a larger time spent on one frequency step for a good reliability of the velocity measurement. This demands a faster settling time for the signal generator. The SRI can be increased beyond which there is insignificant improvement in the accuracy,
2) A trade-off between measurement time and accuracy.

Table I outlines the radar system parameters specific to the SFCW configuration. $Matlab$ simulations were conducted to evaluate the fluctuations in range uncertainty (as defined in (23)) and velocity uncertainty (as described in (28)). These simulations involved varying both range and T_{sw} values across different RCS, as illustrated in Fig. 2c and Fig. 2d, respectively.

III. Effect of PLL RMS Jitter

In [10], phase error represented by the power spectral density (PSD), $S_{\phi,out}(f)$, of the receiver output phase, $\phi_{out}(t)$, was presented. However, it did not explicitly report the effect in range and velocity error because of the inherent PLL RMS jitter. The analysis covered in this section relates the range and velocity error for both the FMCW and SFCW radars because of the PLL RMS jitter, denoted as σ_T. Also, if the PLL is not over-designed to improve its σ_T, the radar system can still maintain its uncertainties in measurement within limits by choosing an appropriate sweeping time or SRI.

A. FMCW

If σ_T denotes the RMS jitter of the PLL integrated over some bandwidth, then in this section, we will show how the range and velocity uncertainty are related to the specifications of the PLL. Neglecting $1/f$ noise, the standard deviation of the receiver output of period, T_o, is given in [10] as

$$\sigma_{To} = \sqrt{2}\sigma_T. \tag{29}$$

With $f_o = 1/T_o$, (29) and PoU we get,

$$\sigma_{fo} = f_o \frac{\sigma_T}{T_o} = \sqrt{2}\sigma_T.f_o^2 \tag{30}$$

The number of oscillations of the output signal in one sweep T_{sw} is given as $n = T_{sw} f_o$. Therefore, the standard deviation of the average IF frequency within one sweep is given as

$$\sigma_{\bar{f}o} = \sqrt{\frac{2}{T_{sw}}}.\sigma_T.f_o^{1.5} \tag{31}$$

1) Range uncertainty: Applying PoU on the range relation to B, T_{sw} given in (2) we get

$$\sigma_R = \frac{T_{sw}.c_o}{2B}.\sigma_{\bar{f}o} \tag{32}$$

Putting (31) and (2) in (32), we get the standard deviation in the range in terms of PLL RMS jitter σ_T, R, B and T_{sw}.

$$\sigma_R = \sqrt{\frac{B}{c_o}}\frac{2\sigma_T}{T_{sw}}.R^{1.5} \tag{33}$$

Below are the conclusions drawn from the above study:

1) With $\sigma_R \propto \frac{R^{1.5}\sigma_T}{T_{sw}}$, a smaller range uncertainty demands a smaller jitter and a larger chirp time,
2) a larger chirp time brings a trade-off between the measurement time and accuracy, thus demanding a faster settling time.

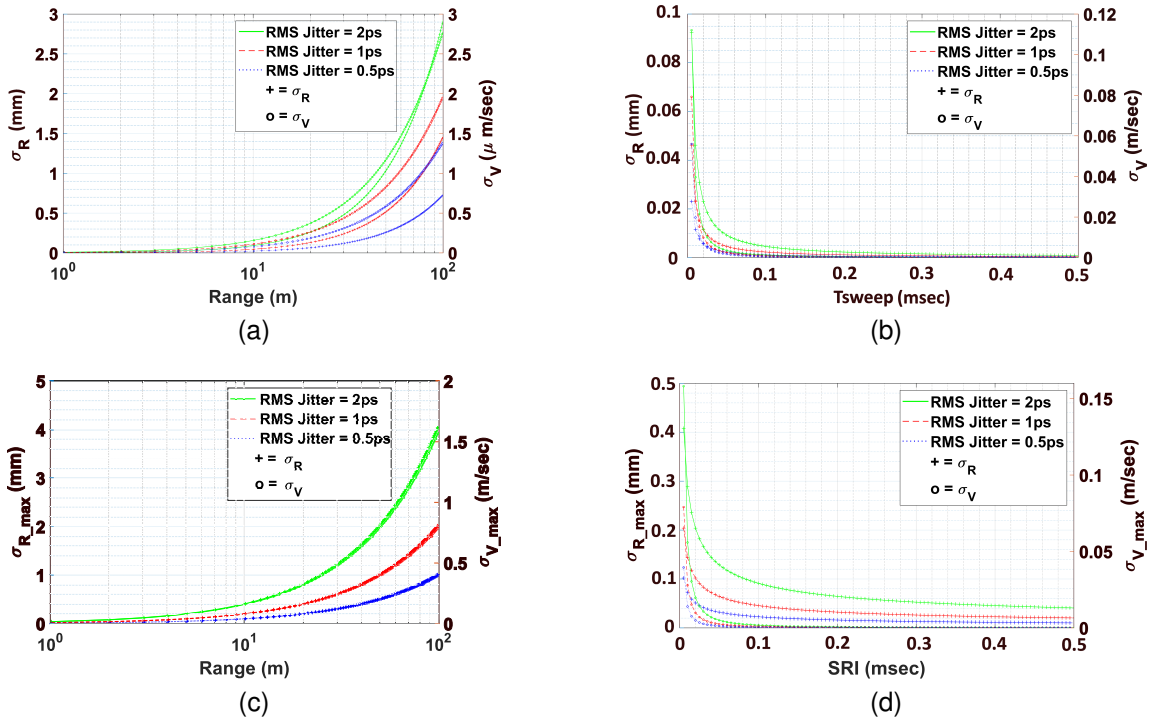

Fig. 3. Effect of σ_T in the receiver in FMCW radar: Range and velocity uncertainty vs (a) range; (b) sweep time, for $R = 10m$. Effect of σ_T in the receiver in SFCW radar: Range and velocity uncertainty vs (a) range; (b) SRI, for $R = 10m$.

2) Velocity uncertainty: Similar to the assumptions mentioned in Section II-A2 and the analysis presented to estimate the velocity uncertainty because of the receiver noise, we find the effect on velocity measurement due to the PLL RMS jitter. Using (15), (16), (18), and (33) we get the standard deviation in velocity as

$$\sigma_v = \frac{4\sigma_T}{f_c.T_{sw}^3}\sqrt{\frac{B^3.R^5}{c_o^3}}, \tag{34}$$

where, f_c is the centre frequency. The observations drawn from the study are:

1) With $\sigma_v \propto \frac{R^{2.5}\sigma_T}{T_{sw}^3}$, better accuracy in the velocity measurement requires a small RMS jitter from the PLL along with a long time of chirp,
2) With fixed bandwidth, a trade-off exists between the measurement time and the accuracy, thus demanding a faster settling time.

Equation (33) is coherent with the findings in [10]. The $Matlab$ simulations for the variation of range uncertainty (in (33)) and velocity uncertainty (in (34)) with range and T_{sw} for different values of PLL RMS jitter are shown in Fig. 3a and Fig. 3b, respectively. The standard deviation in both range and velocity increases for far-field objects and higher σ_T. In contrast, the standard deviation in range and velocity decreases with an increase in T_{sw}.

B. SFCW

The subsequent subsections will cover the variance in range and velocity because of the PLL RMS jitter, σ_T, in SFCW radar measurement.

1) Range uncertainty: Using the relation of phase, $\phi_k = 4\pi f_k R/c$, where $k \in [1, N]$, we infer that the variation in ϕ_k is dependent on the variation in f_k and R. Using the PoU in ϕ_k, we get

$$\frac{\sigma_{\phi_k}^2}{\phi_k^2} = \frac{\sigma_{f_k}^2}{f_k^2} + \frac{\sigma_R^2}{R^2} \tag{35}$$

Using $\phi_k = 4\pi f_k R/c$, and simplifying (35), we get

$$\sigma_{\phi_k}^2 = \frac{(4\pi)^2}{c_o^2}\left[\sigma_{f_k}^2 R^2 + \sigma_R^2 f_k^2\right] \tag{36}$$

Also, the variance in phase relates to the variance in PLL RMS jitter as $\sigma_{\phi_k}^2 = (2\pi)^2 f_k^2 \sigma_T^2$. When the measurement is taken for N number of stepped frequencies, the resulting variance gets divided by N. Using (31) and the above relation of variance in phase, (36) can be represented as

$$\left(4\pi^2.f_k^2.\sigma_T^2 + \frac{16\pi^2.R^2}{c_o^2.N}\frac{2.f_k^3.\sigma_T^2}{(SRI)}\right) = \frac{16\pi^2.\sigma_R^2.f_k^2}{c_o^2.N} \tag{37}$$

The SFCW radars are widely used in short-range applications. Therefore, for small range, $4\pi^2 f_k^2 \sigma_T^2 << \frac{16\pi^2.R^2}{c_o^2.N}\frac{2f_k^3.\sigma_T^2}{(SRI)}$. Thus, we get the variance in range measurement as

$$\sigma_{R\_max}^2 = \frac{2R^2.f_{max}.\sigma_T^2}{(SRI)} \tag{38}$$

The conclusion drawn from (38) are mentioned below:

1) $\sigma_{R\_max} \propto \frac{R.f_{max}^{0.5}.\sigma_T}{\sqrt{(SRI)}}$ demands a small RMS jitter from the signal generator and a larger SRI, for a faithful accuracy in the range measurement,
2) for a fixed RMS jitter, a trade-off exists between measurement time and accuracy, thus demanding a faster settling time.

2) Velocity uncertainty: For an SFCW radar, the phase difference at f_k over two consecutive bursts is represented in (24) for the first frequency step f_1. Using PoU, the variation in ϕ_d will be the sum of variations in frequency f_k and timing difference Δt and given as

$$\frac{\sigma^2_{\phi_d}}{\phi^2_d} = \frac{\sigma^2_{f_k}}{f^2_k} + \frac{\sigma^2_{\Delta t}}{\Delta t^2} \tag{39}$$

Expanding (39) and taking an average of N samples, we get

$$\sigma^2_{\phi_d} = 4\pi^2 N^2 \left[\Delta t^2 \sigma^2_{f_k} + f^2_k \sigma^2_{\Delta t}\right] \tag{40}$$

Using the variance of v representation in (26), and Equation (40), we get

$$\sigma^2_v = \frac{c^2_o}{2.(N.SRI)^2}\left[\frac{\Delta t^2.f_k}{(N.SRI)} + \frac{1}{2}\right].\sigma^2_T \tag{41}$$

Since $\frac{\Delta t^2 f_k}{SRI} >> \frac{1}{2}$, the second term in (41) can be ignored. Taking into consideration the assumptions mentioned in Section II-A2 and using Equation (24), we get the maximum variance in the velocity as,

$$\sigma^2_{v\_max} = \frac{2R^2.f_{max}}{(N.SRI)^3}.\sigma^2_T \tag{42}$$

The conclusion drawn from (42) are:

1) $\sigma_{v\_max} \propto \frac{R.f^{0.5}_{max}}{(SRI)^{1.5}}.\sigma_T$ demands a small RMS jitter from the signal generator and a larger SRI, for a faithful accuracy in the velocity measurement,
2) For a fixed RMS jitter, a trade-off exists between the measurement time and accuracy, thus demanding a faster settling time.

The variation of range uncertainty (in (38)) and velocity uncertainty (in (42)) to the range and SRI for different values of PLL RMS jitter in $Matlab$ are shown in Fig. 3c and Fig 3d, respectively.

IV. Measurement Results

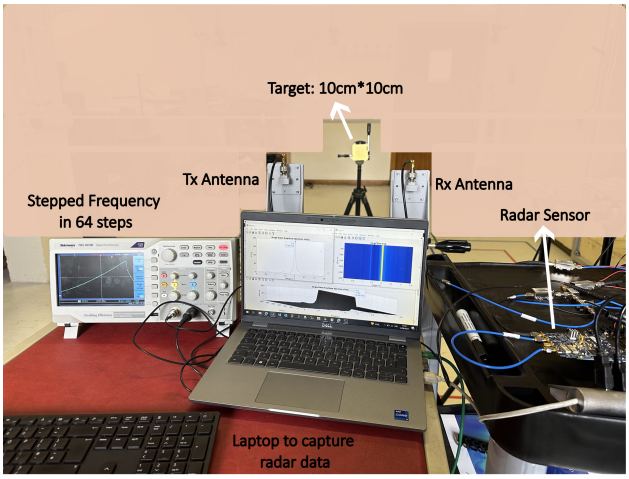

Fig. 4. The experimental setup for range measurement using radar system.

A. Range Measurement with FMCW and SFCW Radar

The measurement was carried out to verify the accuracy derived in theory for the range uncertainty in FMCW and SFCW radars. The experimental set-up is shown in Fig. 4. The parameters of the radar system used for all the measurements are mentioned in Table I. It uses horn antennas for transmitting and receiving signals. The radar system uses commercial off-the-shelf components like ADF4159 as PLL, AD-FMCDAQ2-EBZ as data-acquisition board, Minicircuits ZX60-123LN-S+ as LNA, Genesys-2 board for signal processing and post processing on $Matlab$ through giga byte ethernet. The total power of the radar system is around 5.3 W.

For range measurement, an object of $10\times10\,cm^2$ was attached to a tripod at a distance of 3 m. For the FMCW radar system with a chirp of 1 GHz/50 μs and an ADC sampling rate (f_s) of 100 MHz, the number of samples (N) are 5000 with the frequency resolution of f_s/N = 20 kHz. To investigate the combined effect of the receiver thermal noise and the PLL jitter, the distance measurement was repeated 300 times. The error distribution was fitted with the Gaussian distribution, as shown in Fig. 5(a). The standard deviation in the range measurement is observed to be around 158 μm. Putting the radar system parameters in equations (14) and (33), respectively, results in the total range uncertainty of around 126 μm in the standard deviation owing to the combined effect of receiver thermal noise and PLL RMS jitter. Of 126 μm range uncertainty, the receiver thermal noise contributes around 80%, whereas the PLL RMS jitter contributes around 20%. The impact of receiver thermal noise on a longer range object surpasses the contribution of PLL RMS jitter, aligning with the results reported in [10].

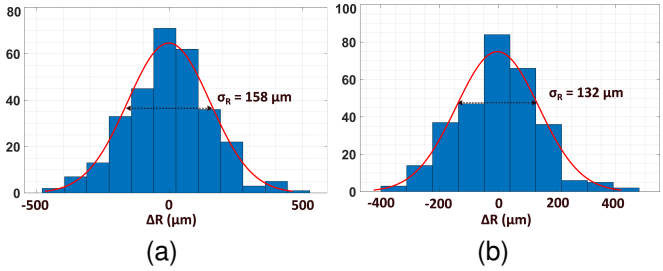

Fig. 5. Histogram for measured error values in range measurement at R=3 m; (a) FMCW (b) SFCW.

A similar setup with radar in SFCW mode (as shown in Fig. 4) was used to find the variance in range. To investigate the combined effect of the receiver thermal noise and the PLL jitter, the distance measurement was repeated 300 times. Figure 5(b) shows the error distribution fitted with the Gaussian distribution. The standard deviation in the range from the measurement is around 132 μm. The theory presented for range uncertainty related to receiver thermal noise and PLL RMS jitter from (23) and (38), respectively, results in the combined effect of around 106 μm. Of 106 μm range uncertainty, the receiver thermal noise contributes around 82%, and the PLL RMS jitter contributes around 18%. The major difference between the measurement and theoretical values for both the above measurements can be attributed to the variance

TABLE II
COMPARISON WITH OTHER PUBLISHED WORKS

	[10]	[12]	[14]	[13]	This Work
Noise Modelled as	VCO noise as OU process	PLL noise as ACN process	PLL noise as Filter-based technique	VCO noise as Leeson's equation	PLL noise as RMS jitter
Range Uncertainty Analysis	Yes	No	Yes	Yes	Yes
Velocity Uncertainty Analysis	No	No	No	No	Yes
FMCW/SFCW Radar Analysis	FMCW	FMCW	FMCW	FMCW	FMCW+SFCW

caused by the sampling clock, which is discussed in Section IV-C.

B. Velocity Measurement with FMCW and SFCW Radar

The measurement was carried out to verify the accuracy derived in theory for the velocity uncertainty in both the FMCW and SFCW radars. The experimental set-up for velocity measurement is shown in Fig. 6 using a 3D printer with the target of $10\times10\,cm^2$ attached to the printer rotary head. The speed of the stepper motor used in the 3D printer is controlled through commands. To investigate the combined effect of the receiver thermal noise and the PLL jitter on the FMCW radar, the velocity measurement was repeated 300 times. The error distribution was fitted with the Gaussian distribution, as shown in Fig. 7(a). The standard deviation in the velocity from the measurement is around 1 nm/sec. The theory presented for velocity uncertainty related to receiver thermal noise and PLL RMS jitter from (19) and (34), respectively, results in the combined effect of around 0.875 nm/sec in the standard deviation. Of this 0.875 nm/sec velocity uncertainty, the receiver thermal noise contributes around 88%, whereas the PLL RMS jitter contributes around 12%.

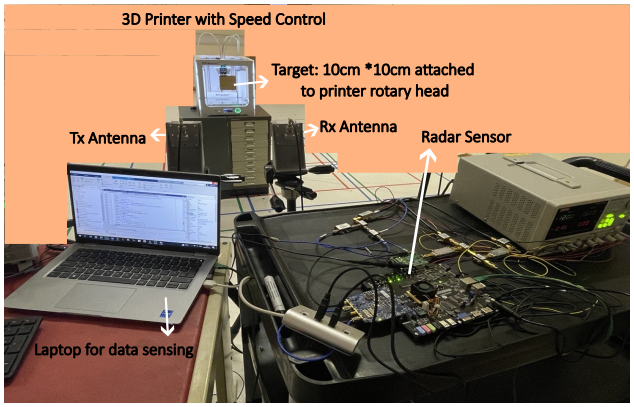

Fig. 6. The experimental setup for velocity measurement using a radar system.

A similar setup with radar in SFCW mode (as shown in Fig. 6) was used to find the uncertainty in velocity measurement. To investigate the combined effect of the receiver thermal noise and the PLL jitter, the velocity measurement was repeated 300 times. The error distribution was fitted with the Gaussian distribution, as shown in Fig. 7(b). The standard deviation in the velocity from the measurement is around 1 μm/sec. The theory presented for velocity uncertainty related to receiver thermal noise and PLL RMS jitter from (28) and (42), respectively, results in the combined effect of around 0.8 μm/sec in the standard deviation. Of this 0.8 μm/sec velocity uncertainty, the receiver thermal noise contributes around 90%, whereas the PLL RMS jitter contributes around 10%. The difference in the measurement and the theoretical values for both the above measurements can again be attributed to the variance caused by the sampling clock, discussed in Section IV-C.

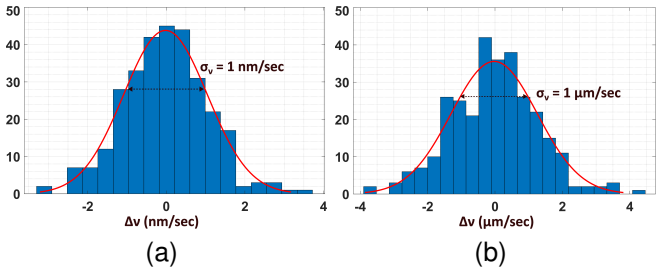

Fig. 7. Histogram for measured error values in velocity measurement at R=3 m and ν=1 mm/sec; (a) FMCW (b) SFCW.

C. Discussion on the Measured Results

Total noise power in the sampled IF signal at the radar output, $(\aleph_{total})$, [21]-[23], is given as

$$\aleph_{total} \approx \aleph_{\mathcal{L}_{IF}} + \aleph_{\mathcal{L}_{fs}} \tag{43}$$

where the first term represents the noise power associated with the IF signal, while the subsequent term corresponds to the noise power attributed to the ADC's sampling clock.

Based on Equation (43), the RMS jitter of the sampling clock was monitored separately using the eye diagram. The measured RMS jitter of the sampling clock, when plugged in equations (33) and (38), resulted in the range standard deviation of 30 μm and 23 μm respectively. The measured RMS jitter of the sampling clock, when used in equations (34) and (42), resulted in a velocity standard deviation of 0.122 nm/sec and 0.09 μm/sec, respectively. Hence, the mismatch in the measurement and theoretical values can be ascribed to the influence of sampling clock jitter, which is beyond the scope of this work. The other effect, like the power supply-induced error, is not taken into consideration in this work and contributes negligibly. The measurement setup couldn't verify receiver thermal noise and RMS jitter separately due to limitations in isolating these factors independently.

Table II presents a comparative analysis of the methods utilized and the findings presented in this work in comparison

to other published works. It is worth highlighting that in other literature, the explicit correlation between uncertainty and radar parameters is not established. In applications such as advanced driver assistance systems (ADAS), surveillance, and bio-medical, absolute precision may not be of utmost importance, while prioritizing rapid measurements becomes essential. The outcomes of this study affirm that choosing an appropriate settling time for the signal generator aligns with the requisite accuracy level in these applications. The necessity for fast measurements emphasizes the importance of incorporating a fast-settling PLL in radar used in Industry 4.0.

V. Conclusion

The paper presented the influence of noise on the range and velocity measurement of FMCW and SFCW radars. The receiver thermal noise has a greater effect on a longer-range target. The work also investigated the effect of PLL RMS jitter, σ_T, on the measurement error. The need to over-design the PLL for lower σ_T can be compensated by choosing a fast settling PLL with a proper chirp time or SRI of the radar system. With these dependencies known apriori, the system designer can estimate the effect of the specifications of the signal generator in developing a robust radar system. The theory provided has been validated with the measurement from a radar in X-band. The measurement accuracy is in the same order as the theoretical value derived in this work. The minuscule difference between the theoretical and the measured values can be attributed to other noise sources, which are beyond the scope of this work.

References

[1] G. C. George, J. J. U. Buch, A. Prince A and S. K. Pathak, "SoC-Based Automated Diagnostic Instrument for FMCW Reflectometry Applications," *IEEE Trans. Instrum. Meas.,* vol. 70, pp. 1-11, 2021.

[2] Z. Li, T. Jin, Y. Dai and Y. Song, "Motion-Robust Contactless Heartbeat Sensing Using 4-D Imaging Radar," *IEEE Trans. Instrum. Meas.,* vol. 72, pp. 1-10, 2023.

[3] F. Khan, S. Azou, R. Youssef, P. Morel, E. Radoi and O. A. Dobre, "An IR-UWB Multi-Sensor Approach for Collision Avoidance in Indoor Environments," *IEEE Trans. Instrum. Meas.,* vol. 71, pp. 1-13, 2022.

[4] G. Tiwari and S. Gupta, "An mmWave Radar Based Real-Time Contactless Fitness Tracker Using Deep CNNs," *IEEE Sensors J.,* vol. 21, no. 15, pp. 17262-17270, 1 Aug.1, 2021.

[5] B. Annino, "Low Phase Noise DAC-Based Frequency Synthesis for Fast Hopping Wideband Microwave Applications", 2021. [Online]. Available: Analog.com [Accessed: July 2021].

[6] J. Wu, Y. Ma, J. Zhang and M. Xie, "A Low-Jitter Synchronous Clock Distribution Scheme Using a DAC Based PLL," *IEEE Trans. Nucl. Sci.,* vol. 57, no. 2, pp. 589-594, April 2010.

[7] J. Xiao, N. Liang, B. Chen and M. Liu, "An 8.55–17.11-GHz DDS FMCW Chirp Synthesizer PLL Based on Double-Edge Zero-Crossing Sampling PD With 51.7-fsrms Jitter and Fast Frequency Hopping," *IEEE Trans. Very Large Scale Integr. (VLSI) Syst.*, vol. 30, no. 3, pp. 267-276, March 2022.

[8] D. -C. Kim et al., "High-Resolution Digital Beamforming Receiver Using DDS–PLL Signal Generator for 5G Mobile Communication," *IEEE Trans. Antennas and Propag.,* vol. 70, no. 2, pp. 1428-1439, Feb. 2022.

[9] W. Wu, R. B. Staszewski and J. R. Long, "A 56.4-to-63.4 GHz Multi-Rate All-Digital Fractional-N PLL for FMCW Radar Applications in 65 nm CMOS," *IEEE J. Solid-State Circuits,* vol. 49, no. 5, pp. 1081-1096, May 2014.

[10] F. Herzel, D. Kissinger and H. J. Ng, "Analysis of Ranging Precision in an FMCW Radar Measurement Using a PLL," *IEEE Trans. Circuits Syst. I, Reg. Papers,* vol. 65, no. 2, pp. 783-792, Feb. 2018.

[11] A. Ergintav, F. Herzel, G. Fischer and D. Kissinger, "A Study of Phase Noise and Frequency Error of a Fractional-N PLL in the Course of FMCW Chirp Generation," *IEEE Trans. Circuits Syst. I, Reg. Papers,* vol. 66, no. 5, pp. 1670-1680, May 2019.

[12] P. Tschapek et al., "A Novel Approach for Modeling and Digital Generation of RF Signals Distorted by Bandlimited Phase Noise," *IEEE J. Microwaves,* vol. 2, no. 4, pp. 699-710, Oct. 2022.

[13] M. Dudek et al., "The impact of phase noise parameters on target signal detection in FMCW-radar system simulations for automotive applications," *Proc. IEEE CIE Int. Conf. Radar (Radar),* Chengdu, China, 2011, pp. 494-497.

[14] D. Dhar et al., "Modeling and analysis of the effects of PLL phase noise on FMCW radar performance," *Proc. IEEE Int. Symp. Circuits Syst. (ISCAS),* Baltimore, MD, USA, 2017, pp. 1-4.

[15] W. Kester, "Converting Oscillator Phase Noise to Time Jitter", 2008. [Online]. Available: Analog.com [Accessed: Oct. 2021].

[16] Y. Zhang, D. Huston and T. Xia, "Signal Calibration and Noise Reduction for Software-Defined Radio-Based GPR," *IEEE Trans. Instrum. Meas.*, vol. 72, pp. 1-10, 2023, Art no. 8000110.

[17] L. Qiao et al., "Learning-Refined Integral Null Space Pursuit Algorithm for Noncontact Multisubjects Vital Signs Measurements Using SFCW-UWB and IR-UWB Radar," *IEEE Trans. Instrum. Meas.*, vol. 71, pp. 1-13, 2022, Art no. 8506013.

[18] S.-E. Hamran, D.T. Gjessing, J. Hjelmstad, E. Aarholt, "Ground penetrating synthetic pulse radar: dynamic range and modes of operation," *J. Appl. Geophys.,* vol. 33, no. 1–3, pp. 7-14, Jan. 1995.

[19] Texas Instruments, "The Fundamentals of Millimeter Wave Radar Sensor," SPYY005A, 2020 [Online:TI.com].

[20] Merrill I. Skolnik, "Radar Handbook," July, 2008.

[21] K. Siddiq, M. K. Hobden, S. R. Pennock and R. J. Watson, "Phase Noise in FMCW Radar Systems," *IEEE Trans. Aerosp. Electron. Syst.,* vol. 55, no. 1, pp. 70-81, Feb. 2019.

[22] K. Siddiq, R. J. Watson, S. R. Pennock, P. Avery, R. Poulton and S. Martins, "Analysis of sampling clock phase noise in homodyne FMCW radar systems," in *Proc. IEEE Radar Conf. (RadarConf),* Philadelphia, PA, USA, 2016, pp. 1-4.

[23] C. Azeredo-Leme, "Clock Jitter Effects on Sampling: A Tutorial," *IEEE Circuits Syst. Mag.,* vol. 11, no. 3, pp. 26-37, Aug 2011.

Zeeshan Ali is currently a post-doctorate researcher in MeLab at the University of Glasgow, Glasgow, UK. He received the M.Tech. degree in electrical engineering from IIT Delhi, New Delhi, India, in 2017 and the Ph.D. degree at the Department of Electrical Engineering, IIT Bombay, Mumbai, India, in 2023. His research interests include analog/digital frequency synthesizers, mixed-signal and cryo-CMOS based circuit design.

Mostafa Elsayed is currently working toward a Ph.D. degree at James Watt School of Engineering, University of Glasgow, Glasgow, UK. His research interests include radar systems design, radar signal processing, RF frequency synthesizers, and mixed-signal circuit design.

Girish Tiwari received the M.Tech and Ph.D. degrees in Electrical Engineering from the Indian Institute of Technology Bombay in 2022. His research interests include radar systems, radar signal processing, applied machine/deep learning and analog circuits design.

Meraj Ahmad received the M.Tech + Ph.D. (Dual Degree) from the Indian Institute of Technology Bombay in 2021. He is currently a post-doctorate fellow in MeLab at the University of Glasgow, Glasgow, UK. His research interests include analog circuit design and embedded system design for sensing applications.

Julien Le Kernec received the B.Eng. and M.Eng. degrees in electronic engineering from Cork Institute of Technology, Cork, Ireland, in 2004 and 2006, respectively, and the Ph.D. degree in electronic engineering from the University Pierre and Marie Curie, Paris, France, in 2011. He is currently a Senior Lecturer with the School of Engineering, University of Glasgow, Glasgow, U.K. He is also a Senior Lecturer with the University of Electronic Science and Technology of China, Chengdu, China, and an Adjunct Associate Professor with the ETIS Laboratory, University of Cergy–Pontoise, Cergy, France.

Hadi Heidari is currently a Professor of nanoelectronics with the James Watt School of Engineering, University of Glasgow, Glasgow, UK, where his Microelectronics Laboratory (meLAB) conducts pioneering research on integrated microelectronics/nanoelectronics design for medical (wearables and implantables) and industrial (quantum computing and ultrasound systems) applications. His research has been funded circa $11M$ by major research councils and funding organizations, including the U.K. Research and Innovation (UKRI) (the Engineering and Physical Sciences Research Council (EPSRC) and Innovate UK), the European Commission, the Royal Society, British Council, the Scottish Funding Council, and the Royal Society of Edinburgh.

Shalabh Gupta received B. Tech degree from the Indian Institute of Technology Kanpur (in 2001), and MS and PhD degrees from UCLA, all in Electrical Engineering. He has worked in industry and academia in the areas of high-speed analog/RF integrated circuits, ultra-fast data conversion using optical techniques, and high-capacity coherent optical links. Since 2009, he has been with the Indian Institute of Technology Bombay, where he is currently a Professor of Electrical Engineering. His current research interests include electronic and photonic integrated circuits and systems for wired, wireless and optical communications, and more specifically, high-speed interconnects.